

1 **Fabrication of free-standing silicon carbide on silicon microstructures via**
2 **massive silicon sublimation**

3 Mojtaba Amjadipour¹, Jennifer MacLeod², Nunzio Motta², and Francesca Iacopi^{1*}

4 ¹ School of Electrical and Data Engineering, Faculty of Engineering and Information
5 Technology, University of Technology Sydney, NSW, Australia

6 ² School of Chemistry and Physics, Science and Engineering Faculty, Queensland University of
7 Technology (QUT), QLD, Australia

8 * Electronic mail: francesca.iacopi@uts.edu.au

9 **Abstract**

10 Heteroepitaxial thin films of cubic silicon carbide (3C-SiC) on silicon offer a promising platform
11 for leveraging the properties of SiC, such as a wide bandgap, high mechanical strength, and
12 chemical stability, on a silicon substrate. Such heteroepitaxial films also attract considerable
13 interest as pseudo-substrates for the growth of GaN as well as graphene on silicon wafers.
14 However, due to a substantial lattice mismatch, the growth of 3C-SiC on silicon leads to a
15 considerable amount of stresses, defects and diffusion phenomena at the heterointerface. We
16 show here that the extent of such interface phenomena and stresses is so large that after
17 patterning of the SiC, a massive sublimation of the silicon underneath the SiC/Si interface is
18 promoted via a high temperature anneal, either in high or medium vacuum ambient. A micron-
19 thick air gap can be formed below the SiC structures, making them suspended. Hence, the
20 described approach can be used as a straightforward methodology to form free-standing silicon
21 carbide structures without the need for wet or anisotropic etching and could be of great interest

1 for devices where suspended moving parts are needed, such as micro- and nano-
2 electromechanical systems.

3 **I. Introduction**

4 Heteroepitaxial 3C-SiC/Si has considerable potential for a variety of applications such as micro-
5 electro-mechanical systems (MEMS), high-voltage, high-frequency diodes, and transistors ¹⁻⁴. In
6 addition, the epitaxial graphene growth on SiC on silicon enables direct graphene growth on Si
7 wafers, which makes it compatible with semiconductor industry fabrication methods ⁵⁻⁷. This
8 methodology eliminates the need for transferring graphene to a semiconductor substrate, as is
9 required following chemical vapor deposition (CVD) on a metal or for exfoliated graphite ^{6, 8}.
10 GaN growth on the 3C-SiC/Si pseudo-substrates also has the potential interest for electronics and
11 optoelectronics ⁹⁻¹⁰. The use of heteroepitaxial thin films on silicon as opposed to the use of bulk
12 SiC substrates leads to a cost reduction and enhanced micromachining and integration
13 capabilities, which is desired for a variety of applications such as sensors, energy storage, and
14 nanoelectronics ¹¹⁻¹⁶. However, the significant lattice mismatch between SiC and Si substrate,
15 accompanied by atomic inter-diffusion, defects generation, and stress relaxation, adversely affect
16 the stability of the SiC/Si interface ¹⁷⁻¹⁸. Pradeepkumar et al. ¹⁹ reported a significant intermixing
17 at the heterointerface, which takes place at high temperatures either upon SiC growth or
18 subsequent annealing. They pointed out that the high compressive stress concentration at the
19 heterointerface undergoes substantial relaxation above 1000°C, caused by a significant carbon
20 diffusion microns-deep into the silicon substrate. Substantial diffusion of atomic carbon is
21 expected to create considerable amounts of interstitial C in the silicon lattice, leading to a leaky
22 p-n SiC/Si heterojunction as well as propagating compressive stresses deeper into the silicon
23 substrate, microns away from the heterointerface ¹⁹⁻²².

1 Patterning plays a crucial role in semiconductor technologies²³⁻²⁸. We have extensively
2 investigated the epitaxial graphene fabrication on patterned heteroepitaxial thin films of cubic
3 silicon carbide (3C-SiC) on silicon²⁸⁻²⁹. Conventional patterning techniques include
4 photolithography, electron-beam lithography, and focused ion beam (FIB) milling. Fabrication of
5 SiC structures such as microcantilevers and bridges is of great importance in sensing and MEMS
6 applications^{1,30}. Fabricating these structures using 3C-SiC on silicon thin films generally
7 involves patterning the carbide layer followed by chemical wet etching to release the structures
8 from the Si substrate. The wet etching step is quite time-consuming and demands the use of
9 hazardous chemicals^{1,29,31-32}. Therefore, developing a method to eliminate the need for a wet
10 etching would be highly beneficial.

11 Here, we take advantage of the stresses generated microns deep into the silicon substrate and
12 show an alternative path to fabricating suspended microstructures of 3C-SiC on silicon, based on
13 a simple high-temperature anneal after patterning of the silicon carbide film.

14 **II. Experimental Details**

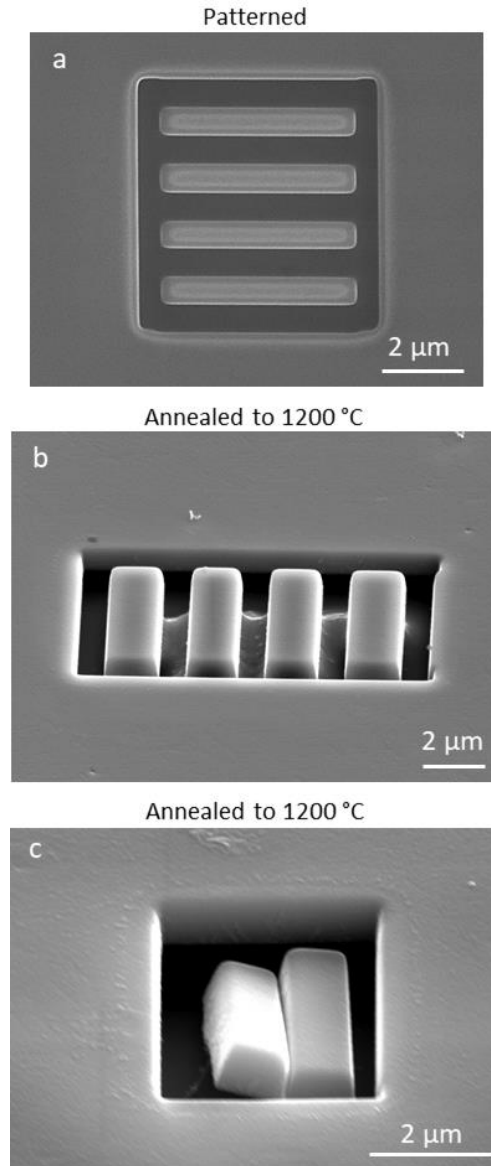
15 3C-SiC films grown on Si(111) and Si(100) were purchased from NOVASIC (France)³³⁻³⁵. The
16 heteroepitaxial growth was carried out in a horizontal hot-wall CVD system at temperatures in
17 the range of 1300-1400 °C by NOVASIC (France)³³. Chemical and mechanical polishing were
18 conducted to reduce the surface roughness to less than 1 nm (StepSiC® by NOVASIC (France))
19³⁶. The cubic polytype of SiC is the only type that can be heteroepitaxially grown on the readily-
20 available, large-diameter silicon substrates³⁷. The wafer was cleaned by successive 10'
21 sonications in acetone, isopropanol, and de-ionized water, respectively.

1 An FEI SCIOS Dual Beam scanning electron microscopy (SEM)/focused ion beam (FIB) system
2 was used for ion-beam patterning the first series of samples. All patterns were fabricated with a
3 Ga beam energy of 30 keV, a dwell time of 1 μ s, a beam overlap of 50 %, and a beam current of
4 0.1 nA. The FEI SCIOS Dual Beam system was also used for scanning transmission electron
5 microscopy (STEM) sample preparation and measurement; beam energies between 2 and 30 keV
6 with a range of beam current from 0.1 to 7 nA were employed. During sample preparation, a Pt
7 layer has been deposited on the area of interest to protect it against unwanted milling. A thin
8 lamella was cut, lifted out, and welded to a copper grid using Pt deposition. The transferred sample
9 was then thinned to about 100 nm thickness to make it transparent to electrons for STEM imaging.
10 High-temperature annealing was conducted using an Omicron Multiprobe system with a base
11 pressure of 10^{-10} mbar. Joule heating was employed for the high-temperature annealing at $1250 \pm$
12 15 °C for 10 minutes. The temperature was controlled using an optical pyrometer (IRCON Ultimax
13 UX-20P with emissivity = 0.9).

14 The cantilever and bridge structures were patterned using electron-beam lithography followed by
15 plasma etching. Poly(methyl methacrylate) (PMMA) 950K was used as the photoresist layer. The
16 resist layer was spin-coated (3000 rpm, 1 minute) and baked (180 °C, 3 minutes). A Zeiss Supra
17 55VP SEM with a beam energy of 15 keV was used for photoresist exposure. A reactive ion etcher
18 with 60 sccm of SF₆ and 100 W power was employed for etching the SiC layer. High-temperature
19 annealing for silicon sublimation was conducted using a Carbolite Gero furnace at ~ 1200 °C for
20 30 minutes with a base pressure of 10^{-6} mbar.

1 **III. Results and Discussions**

2 We investigated the SiC/Si interface of ion-beam patterned 3C-SiC before and after high-
3 temperature annealing. Figure 1 shows SEM images of the SiC thin film in the as-patterned
4 condition (Figure 1a) and after annealing to ~ 1200 °C for 10 minutes (Figure 1b and c). Four
5 parallel structures (~ 1 μm wide and ~ 4 μm long) were ion-beam milled through the SiC layer
6 thickness with a depth of ~ 1 μm (Figure 1a). After high-temperature annealing of the patterned
7 samples, the SiC structures appear close to detached from the underlying substrate (Figure 1b and
8 c). In Figure 1c, the detachment is more obvious due to different sizes and geometry, and produces
9 a displacement of the structures from their original position.



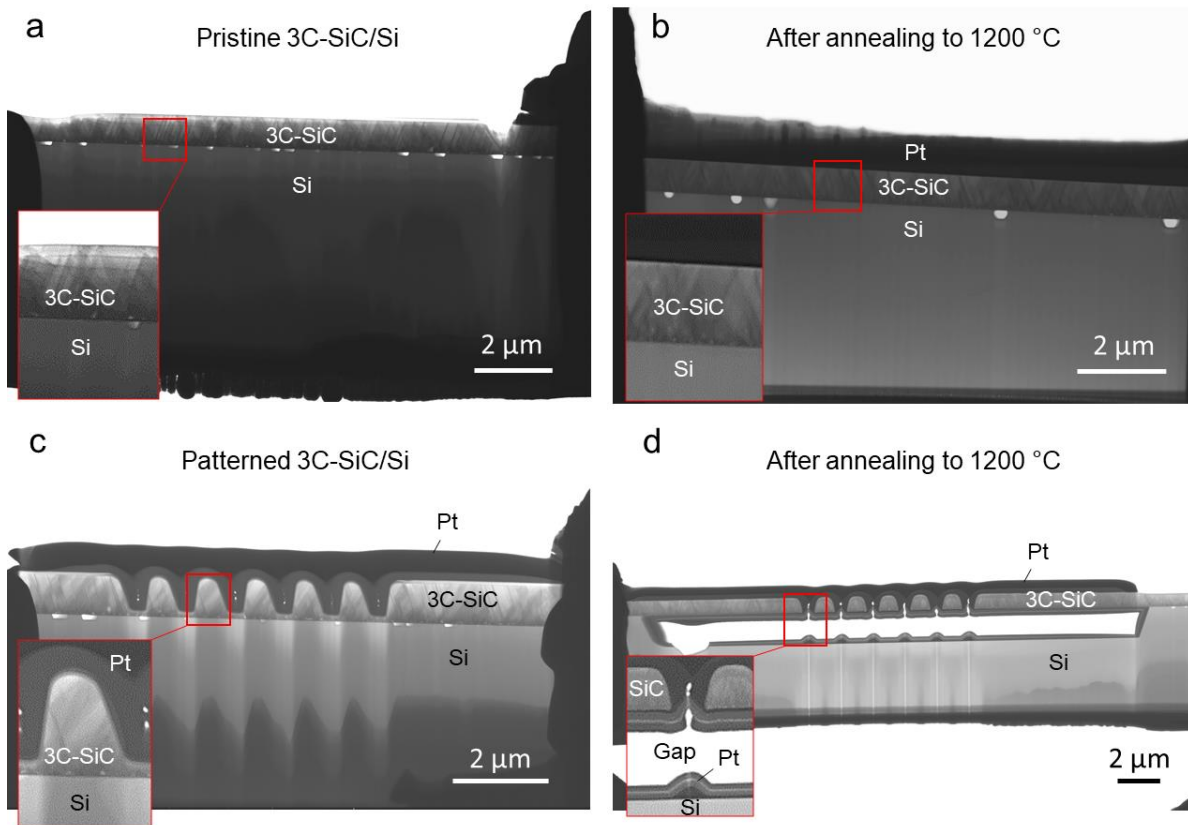
1

2 Figure 1. SEM images (a) pristine 3C-SiC/Si(111) sample patterned with four structures, 1.5 μm
 3 wide and 5 μm long. (b) same patterned sample as in (a) after high-temperature annealing to ~ 1200
 4 $^{\circ}\text{C}$ for 10 minutes. (c) 3C-SiC/Si(111) patterned with structures 1 μm wide and 5 μm long, after
 5 the high-temperature annealing. Note the detachment of the two structures from the substrate.

6 The 3C-SiC/Si interface was further studied with cross-sectional STEM imaging. A pristine 3C-
 7 SiC/Si in as-received condition was investigated before and after the high-temperature annealing.

8 Figure 2a shows the presence of some initial voids at the as-received 3C-SiC/Si interface; these
 9 interfacial voids are caused by silicon out-diffusion during the SiC layer growth and are often

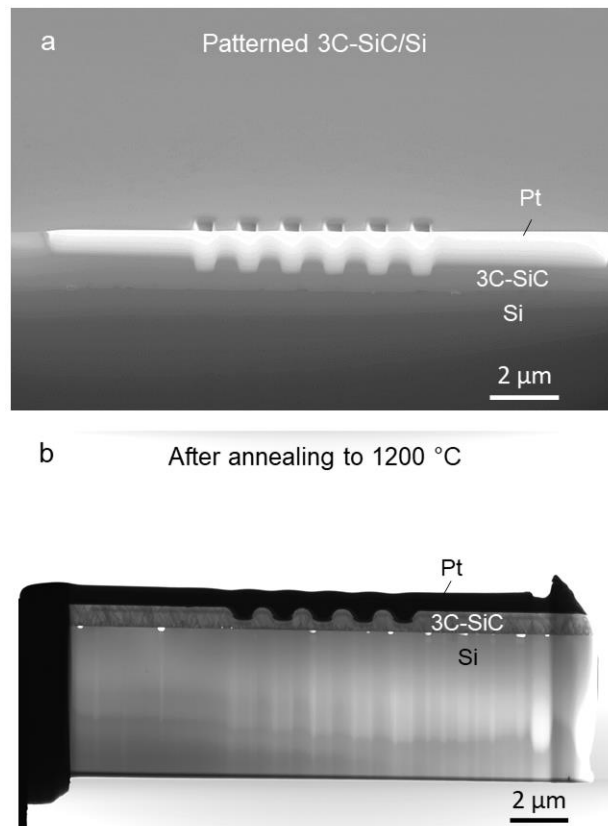
1 visible through microscopy^{20, 38-41}. After annealing the pristine 3C-SiC/Si sample to ~1200 °C for
 2 10 minutes, the average void size at the interface was noticeably larger (Figure 2b). Figure 2c
 3 shows the 3C-SiC/Si sample, with a patterned SiC layer before high-temperature annealing. The
 4 SiC/Si interface for the sample after patterning, and before annealing, appears similar to the as-
 5 received one. However, the annealing of the patterned sample at high temperatures (~1200 °C for
 6 10 minutes) produces a dramatic change (Figure 2d), with the formation of a massive gap between
 7 the SiC and the Si substrate. This gap is strongly anisotropic as it extends for about a micron depth,
 8 and in-plane, up to ~8 μm away from the patterned SiC trenches, as shown in Figure 2d.



9

10 Figure 2. STEM image of 3C-SiC/Si(111) cross-sections (a) for an as-received sample, (b) the
 11 as-received sample after annealing to ~1200 °C for 10 minutes, (c) a patterned 3C-SiC/Si(111),
 12 and (d) the patterned 3C-SiC/Si after annealing to ~1200 °C for 10 minutes.

1 To further investigate this phenomenon, a 3C-SiC/Si sample was patterned with a depth of about
2 only half of the SiC layer thickness ($\sim 0.5 \mu\text{m}$). Following annealing to $\sim 1200 \text{ }^\circ\text{C}$ for 10 minutes,
3 the interface for the sample does not show the formation of an air gap after annealing (Figure 3).
4 This indicates that the massive sublimation can only happen when the regions of the silicon
5 substrate are exposed to the ambient through openings patterned in the SiC layer.



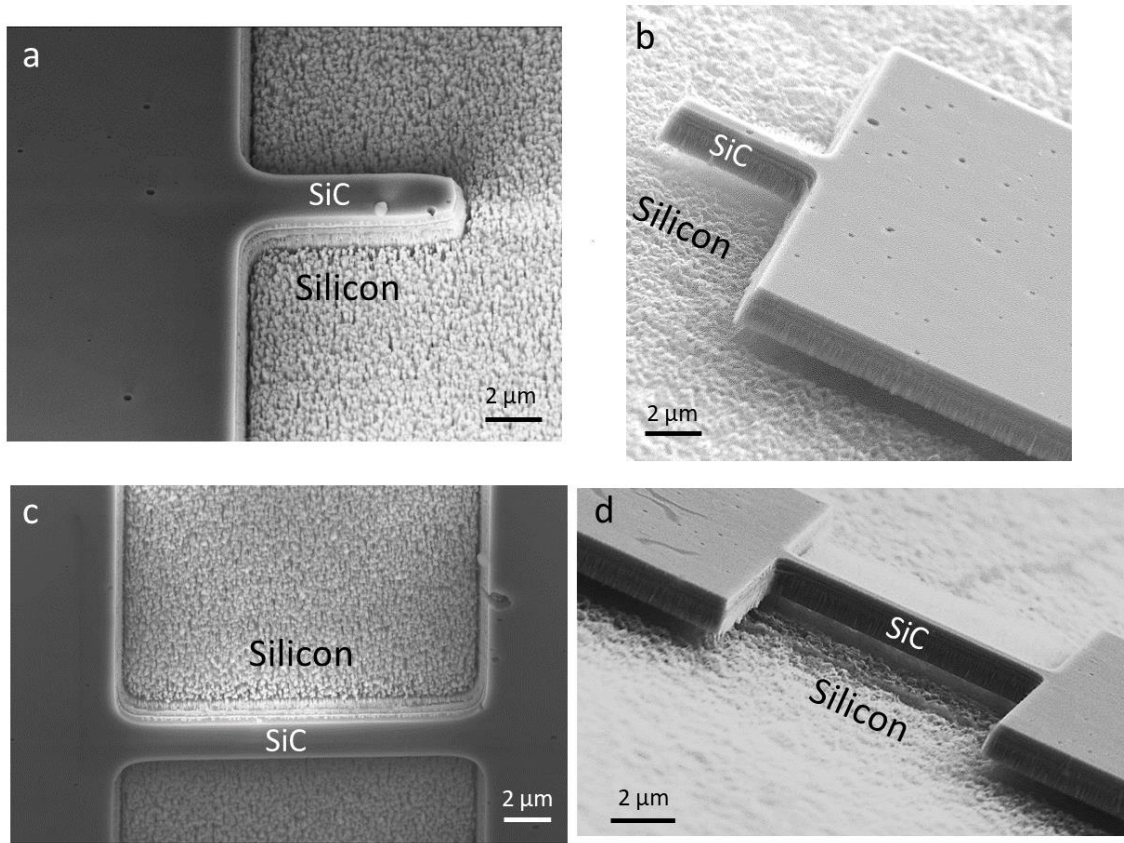
6
7 Figure 3. (a) SEM image of the cross-section of a 3C-SiC/Si(111) film only etched half-way
8 through its thickness, before high-temperature annealing, (b) STEM cross-section image after
9 annealing of the sample to $\sim 1200 \text{ }^\circ\text{C}$ for 10 minutes, indicating no large gap formation under the
10 SiC film, but only small-sized voids.

11 In Figure 4 a and c, we show cantilever and bridge structures of 3C-SiC/Si(100), patterned using
12 electron-beam lithography followed by plasma etching. Figure 4 b and d indicate that after
13 annealing of the patterned samples to $\sim 1200 \text{ }^\circ\text{C}$, the structures appear suspended from the Si
14 substrate. Although a higher amount of stress is expected for the (111) orientation as compared

1 to (100)^{17, 42}, the phenomenon of massive sublimation occurs in both 3C-SiC/Si(100) and 3C-
2 SiC/Si(111) systems. We emphasize once more that this massive sublimation is not observable in
3 samples where the SiC has not been fully opened to expose the silicon substrate.

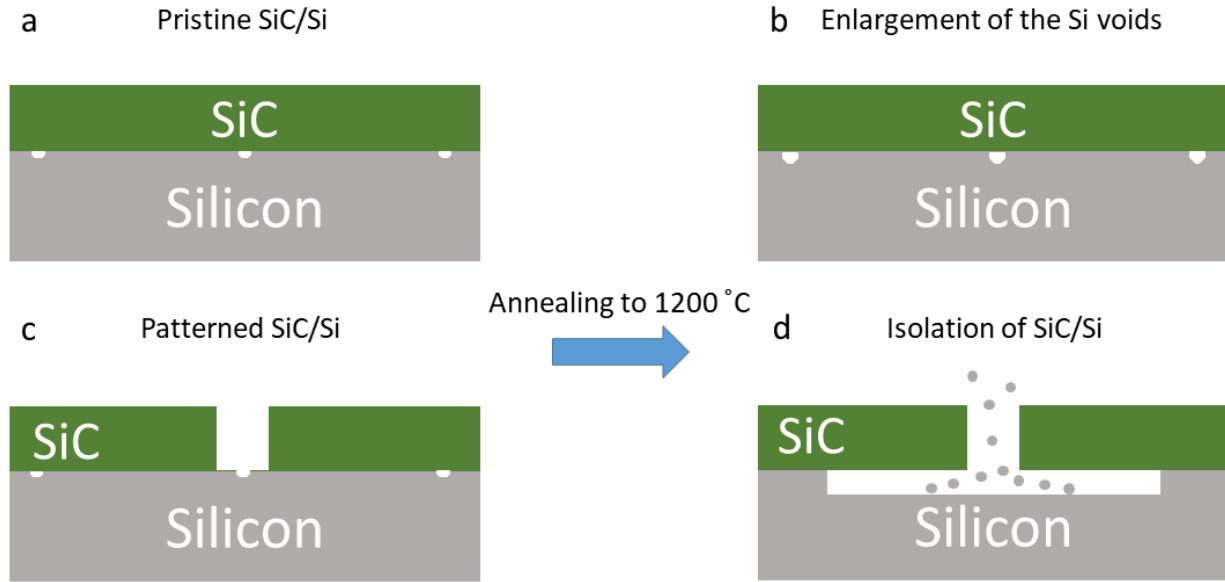
4 The observed phenomenon is hence exemplified in the schematic in Figure 5. The silicon
5 underneath the SiC film is weakened by the compressive stresses discussed earlier, up to microns
6 away from the interface. Therefore, when brought to high temperatures, the silicon in the top
7 portion of the substrate has a strong tendency to sublimate. When a continuous SiC film is
8 present above the substrate, the carbide acts as a barrier, so that a high temperature anneal can
9 only induce small-scale sublimation of the silicon through (Figure 5, a and b). In this case,
10 silicon can only leave the substrate through stacking faults or other defects of the heteroepitaxial
11 SiC⁴¹. When patterns are fully opened in the SiC layer, the surface of the silicon substrate
12 becomes exposed to the ambient (Figure 5c), enabling a massive sublimation upon annealing,
13 and the formation of an anisotropic gap at the interface (Figure 5d). The strong anisotropy of this
14 process is explained by the fact that the compressive stresses underpinning the driving force for
15 this massive sublimation are directly related to the diffusion depth into the silicon of the atomic
16 carbon from the heterointerface, which obeys Fick's law⁴³⁻⁴⁴. The annealing temperature, the
17 annealing time, and the geometry of the microstructures are all expected to affect the formation
18 of the air-gap.

19 This phenomenon can hence be employed to fabricate various suspended SiC structures without
20 any chemical wet-etching. In addition, when necessary, this process may be engineered further to
21 fabricate SiC structures which are electrically insulated from its silicon substrate.



1

2 Figure 4. (a) a cantilever structure patterned on a $\sim 2 \mu\text{m}$ thick SiC/Si(100) thin-film using
 3 electron-beam lithography and plasma etching procedure, (b) the cantilever structure after high-
 4 temperature annealing to $\sim 1200 \text{ }^\circ\text{C}$, a gap has created under the structure. (c) a bridge structure
 5 patterned on SiC/Si substrate using electron-beam lithography procedure, (d) the bridge structure
 6 after high-temperature annealing to $\sim 1200 \text{ }^\circ\text{C}$, a gap has created under the structure.



1
 2 Figure 5. Schematic representation of the patterning effect on the SiC/Si interface after the high-
 3 temperature annealing (a) pristine thin film of SiC/Si with visible interfacial voids sometimes
 4 visible during the SiC growth, (b) after high-temperature annealing: enlargement of the
 5 interfacial voids, (c) patterning of the SiC/Si exposes the silicon to the atmosphere (d) high-
 6 temperature annealing leads to a massive Si sublimation, resulting in the formation of an
 7 anisotropic gap extending for microns.

8 **IV. Conclusions**

9 We have shown that we can induce a massive silicon sublimation underneath the interface of a
 10 heteroepitaxial SiC layer on silicon, by patterning the SiC layer to expose the silicon surface and
 11 annealing the system to either high or medium vacuum ambient. We suggest that the driving
 12 force of this massive sublimation is given by significant compressive stresses generated deep in
 13 the silicon substrate by the presence of interstitial carbon diffused from the heterointerface.

14 This massive sublimation is anisotropic and extends for about a micron depth and several
 15 microns in each in-plane direction from the open SiC pattern, which results in the formation of
 16 an air gap between the SiC structures and the silicon substrate.

1 Employing this phenomenon, we have fabricated free-standing structures of 3C-SiC on a silicon
2 substrate. This process eliminates the need for any chemical etching step to fabricate free-
3 standing SiC structures on Si substrate. We propose this methodology as a pathway to directly
4 fabricate free-standing micro- and nano-structures of crystalline 3C-SiC on silicon, which are,
5 for example, the basis for MEMS resonators with very high-quality factors ⁴⁵⁻⁴⁶. In addition,
6 released structures made of epitaxial graphene on SiC can be fabricated using this process. The
7 epitaxial graphene/SiC material combination is of great relevance and benefit, particularly for
8 mechanical ⁴⁷⁻⁴⁹ and optical/photonic applications ⁵⁰⁻⁵².

9 **Acknowledgments**

10 Funding from the Air Force Office for Scientific Research through grants 18IOA052 is kindly
11 acknowledged. The authors thank the support of the Queensland Government through the Q-
12 CAS Collaborative Science Fund 2016. This work was enabled by the Central Analytical
13 Research Facility hosted by the Institute for Future Environments at QUT and was performed in
14 part at the Queensland node of the Australian National Fabrication Facility. The UTS MAU labs
15 are acknowledged for providing access to the fabrication facilities. We acknowledge the
16 technical support of Dr. Annalena Wolff, Dr. Josh Lipton-Duffin, Dr. Hui Diao, Dr. Mark
17 Lockrey, and Mr. Geoff McCredie.

18 **References**

- 19 ¹P. S. Waggoner, H. G. Craighead, *Lab on a Chip*, **7**, 1238-1255, (2007).
20 ²S. Nishino, Y. Hazuki, H. Matsunami, T. Tanaka, *J. Electrochem. Soc.*, **127**, 2674-2680, (1980).
21 ³J. Casady, R. W. Johnson, *Solid-State Electron.*, **39**, 1409-1422, (1996).
22 ⁴X. She, A. Q. Huang, O. Lucia, B. Ozpineci, *IEEE Transactions on Industrial Electronics*, **64**,
23 8193-8205, (2017).
24 ⁵A. Van Bommel, J. Crombeen, A. Van Tooren, *Surf Sci.*, **48**, 463-472, (1975).

1 ⁶C. Berger, Z. Song, X. Li, X. Wu, N. Brown, C. Naud, D. Mayou, T. Li, J. Hass, A. N.
2 Marchenkov, E. H. Conrad, P. N. First, W. A. De Heer, *Science*, **312**, 1191-1196, (2006).
3 ⁷B. Gupta, M. Notarianni, N. Mishra, M. Shafiei, F. Iacopi, N. Motta, *Carbon*, **68**, 563-572,
4 (2014).
5 ⁸C. Riedl, U. Starke, J. Bernhardt, M. Franke, K. Heinz, *Physical Review B*, **76**, 245406, (2007).
6 ⁹D. As, T. Frey, D. Schikora, K. Lischka, V. Cimalla, J. Pezoldt, R. Goldhahn, S. Kaiser, W.
7 Gebhardt, *Appl. Phys. Lett.*, **76**, 1686-1688, (2000).
8 ¹⁰D. K. Wickenden, K. Faulkner, R. Brander, B. Isherwood, *J. Cryst. Growth*, **9**, 158-164,
9 (1971).
10 ¹¹M. Suemitsu, Y. Miyamoto, H. Handa, A. Konno, *e-Journal of Surface Science and*
11 *Nanotechnology*, **7**, 311-313, (2009).
12 ¹²V. Y. Aristov, G. Urbanik, K. Kummer, D. V. Vyalikh, O. V. Molodtsova, A. B. Preobrajenski,
13 A. A. Zakharov, C. Hess, T. Hänke, B. Buchner, *Nano Lett.*, **10**, 992-995, (2010).
14 ¹³A. Ouerghi, R. Belkhou, M. Marangolo, M. Silly, S. El Moussaoui, M. Eddrief, L. Largeau, M.
15 Portail, F. Sirotti, *Appl. Phys. Lett.*, **97**, 161905, (2010).
16 ¹⁴A. Ouerghi, A. Kahouli, D. Lucot, M. Portail, L. Travers, J. Gierak, J. Penuelas, P. Jegou, A.
17 Shukla, T. Chassagne, *Appl. Phys. Lett.*, **96**, 191910, (2010).
18 ¹⁵B. Gupta, E. Placidi, C. Hogan, N. Mishra, F. Iacopi, N. Motta, *Carbon*, **91**, 378-385, (2015).
19 ¹⁶N. Mishra, J. Boeckl, N. Motta, F. Iacopi, *Physica Status Solidi (a)*, **213**, 2277-2289, (2016).
20 ¹⁷F. Iacopi, R. E. Brock, A. Iacopi, L. Hold, R. H. Dauskardt, *Acta Mater.*, **61**, 6533-6540,
21 (2013).
22 ¹⁸V. Cimalla, J. Pezoldt, O. Ambacher, *J. Phys. D: Appl. Phys.*, **40**, 6386, (2007).
23 ¹⁹A. Pradeepkumar, N. Mishra, A. R. Kermany, J. J. Boeckl, J. Hellerstedt, M. S. Fuhrer, F.
24 Iacopi, *Appl. Phys. Lett.*, **109**, 011604, (2016).
25 ²⁰A. Pradeepkumar, M. Zielinski, M. Bosi, G. Verzellesi, D. K. Gaskill, F. Iacopi, *J. Appl. Phys.*,
26 **123**, 215103, (2018).
27 ²¹A. Pradeepkumar, M. Amjadipour, N. Mishra, C. Liu, M. S. Fuhrer, A. Bendavid, F. Isa, M.
28 Zielinski, H. I. Sirikumara, T. Jayasekera, *ACS Applied Nano Materials*, (2019).
29 ²²N. Motta, F. Iacopi, C. Coletti, *Growing graphene on semiconductors* (Pan Stanford, 2017).
30 ²³Y. M. Lin, C. Dimitrakopoulos, K. A. Jenkins, D. B. Farmer, H. Y. Chiu, A. Grill, P. Avouris,
31 *Science*, **327**, 662-662, (2010).
32 ²⁴M. Sprinkle, M. Ruan, Y. Hu, J. Hankinson, M. Rubio-Roy, B. Zhang, X. Wu, C. Berger, W.
33 A. De Heer, *Nature Nanotechnology*, **5**, 727-731, (2010).
34 ²⁵A. Celis, M. Nair, A. Taleb-Ibrahimi, E. Conrad, C. Berger, W. De Heer, A. Tejada, *J. Phys. D:*
35 *Appl. Phys.*, **49**, 143001, (2016).
36 ²⁶M. Terrones, A. R. Botello-Méndez, J. Campos-Delgado, F. López-Urías, Y. I. Vega-Cantú, F.
37 J. Rodríguez-Macías, A. L. Elías, E. Muñoz-Sandoval, A. G. Cano-Márquez, J.-C. Charlier, H.
38 Terrones, *Nano Today*, **5**, 351-372, (2010).
39 ²⁷Z. Li, F. Chen, *Applied Physics Reviews*, **4**, 011103, (2017).
40 ²⁸M. Amjadipour, M. MacLeod, J. Lipton-Duffin, F. Iacopi, N. Motta, *Nanotechnology*, **28**,
41 345602, (2017).
42 ²⁹B. V. Cunnning, M. Ahmed, N. Mishra, A. R. Kermany, B. Wood, F. Iacopi, *Nanotechnology*,
43 **25**, 325301, (2014).
44 ³⁰J. S. Ponraj, S. C. Dhanabalan, G. Attolini, G. Salviati, *Crit. Rev. Solid State Mater. Sci.*, **41**,
45 430-446, (2016).

1 ³¹H. P. Phan, T. K. Nguyen, T. Dinh, A. Iacopi, L. Hold, M. J. Shiddiky, D. V. Dao, N. T.
2 Nguyen, *Adv. Eng. Mater.*, **20**, 1700858, (2018).
3 ³²S. S. Verbridge, J. M. Parpia, R. B. Reichenbach, L. M. Bellan, H. Craighead, *J. Appl. Phys.*,
4 **99**, 124304, (2006).
5 ³³M. Zielinski, M. Portail, S. Roy, T. Chassagne, C. Moisson, S. Kret, Y. Cordier, *Materials*
6 *Science and Engineering: B*, **165**, 9-14, (2009).
7 ³⁴J. Meziere, M. Ucar, E. Blanquet, M. Pons, P. Ferret, L. Di Cioccio, *J. Cryst. Growth*, **267**,
8 436-451, (2004).
9 ³⁵D. Chaussende, L. Latu-Romain, L. Auvray, M. Ucar, M. Pons, R. Madar In *Large Area DPB*
10 *free (111) β -SiC thick layer grown on (0001) α -SiC nominal surfaces by the CF-PVT method*,
11 *Mater. Sci. Forum*, Trans Tech Publ: 2005; pp 225-228.
12 ³⁶B. Gupta, I. Di Bernardo, P. Mondelli, A. Della Pia, M. G. Betti, F. Iacopi, C. Mariani, N.
13 Motta, *Nanotechnology*, **27**, 185601, (2016).
14 ³⁷L. Wang, S. Dimitrijevic, J. Han, A. Iacopi, L. Hold, P. Tanner, H. B. Harrison, *Thin Solid*
15 *Films*, **519**, 6443-6446, (2011).
16 ³⁸N. Becourt, J. Ponthenier, A. Papon, C. Jaussaud, *Influence of temperature on the formation by*
17 *reactive CVD of a silicon carbide buffer layer on silicon* (Elsevier, 1993), p. 79-84.
18 ³⁹K. C. Kim, C. I. Park, J. I. Roh, K. S. Nahm, Y. H. Seo, *Journal of Vacuum Science &*
19 *Technology A: Vacuum, Surfaces, and Films*, **19**, 2636-2641, (2001).
20 ⁴⁰S. Jiao, Y. Murakami, H. Nagasawa, H. Fukidome, I. Makabe, Y. Tateno, T. Nakabayashi, M.
21 Suemitsu, *Materials Science Forum*, **806**, 89-93, (2015).
22 ⁴¹M. Suemitsu, S. Jiao, H. Fukidome, Y. Tateno, I. Makabe, T. Nakabayashi, *J. Phys. D*, **47**,
23 094016, (2014).
24 ⁴²F. Iacopi, G. Walker, L. Wang, L. Malesys, S. Ma, B. V. Cuning, A. Iacopi, *Appl. Phys. Lett.*,
25 **102**, 011908, (2013).
26 ⁴³J. Pelleg, *Diffusion in ceramics* (Springer, 2016).
27 ⁴⁴A. Paul, T. Laurila, V. Vuorinen, S. V. Divinski, *Thermodynamics, diffusion and the kirkendall*
28 *effect in solids* (Springer, 2014), p. 115-139.
29 ⁴⁵E. Romero, V. M. Valenzuela, A. R. Kermany, L. Sementilli, F. Iacopi, W. P. Bowen, *Phys.*
30 *Rev. Appl.*, **13**, 044007, (2020).
31 ⁴⁶A. R. Kermany, G. Brawley, N. Mishra, E. Sheridan, W. P. Bowen, F. Iacopi, *Appl. Phys.*
32 *Lett.*, **104**, 081901, (2014).
33 ⁴⁷M. Mehregany, C. A. Zorman, *Thin Solid Films*, **355**, 518-524, (1999).
34 ⁴⁸T. Dinh, H. P. Phan, N. Kashaninejad, T. K. Nguyen, D. V. Dao, N. T. Nguyen, *Advanced*
35 *Materials Interfaces*, **5**, 1800764, (2018).
36 ⁴⁹A. R. M. Faisal, H.-P. Phan, T. Dinh, T.-K. Nguyen, N.-T. Nguyen, D. V. Dao, *RSC advances*,
37 **8**, 15310-15314, (2018).
38 ⁵⁰Y. Jiang, J. Li, Z. Zhou, X. Jiang, D. Zhang, *Sensors*, **16**, 1660, (2016).
39 ⁵¹F. Martini, A. Politi, *Appl. Phys. Lett.*, **112**, 251110, (2018).
40 ⁵²P. Rufangura, T. Folland, A. Agrawal, J. D. Caldwell, F. Iacopi, *Journal of Physics: Materials*,
41 (2020).

42

43

44

1 **List of the figure captions**

2 Figure 6. SEM images (a) pristine 3C-SiC/Si(111) sample patterned with four structures, 1.5 μm
3 wide and 5 μm long. (b) same patterned sample as in (a) after high-temperature annealing to ~ 1200
4 $^{\circ}\text{C}$ for 10 minutes. (c) 3C-SiC/Si(111) patterned with structures 1 μm wide and 5 μm long, after
5 the high-temperature annealing. Note the detachment of the two structures from the substrate.

6 Figure 7. STEM image of 3C-SiC/Si(111) cross-sections (a) for an as-received sample, (b) the
7 as-received sample after annealing to ~ 1200 $^{\circ}\text{C}$ for 10 minutes, (c) a patterned 3C-SiC/Si(111),
8 and (d) the patterned 3C-SiC/Si after annealing to ~ 1200 $^{\circ}\text{C}$ for 10 minutes.

9 Figure 8. (a) SEM image of the cross-section of a 3C-SiC/Si(111) film only etched half-way
10 through its thickness, before high-temperature annealing, (b) STEM cross-section image after
11 annealing of the sample to ~ 1200 $^{\circ}\text{C}$ for 10 minutes, indicating no large gap formation under the
12 SiC film, but only small-sized voids.

13 Figure 9. (a) a cantilever structure patterned on a ~ 2 μm thick SiC/Si(100) thin-film using
14 electron-beam lithography and plasma etching procedure, (b) the cantilever structure after high-
15 temperature annealing to ~ 1200 $^{\circ}\text{C}$, a gap has created under the structure. (c) a bridge structure
16 patterned on SiC/Si substrate using electron-beam lithography procedure, (d) the bridge structure
17 after high-temperature annealing to ~ 1200 $^{\circ}\text{C}$, a gap has created under the structure.

18 Figure 10. Schematic representation of the patterning effect on the SiC/Si interface after the
19 high-temperature annealing (a) pristine thin film of SiC/Si with visible interfacial voids
20 sometimes visible during the SiC growth, (b) after high-temperature annealing: enlargement of
21 the interfacial voids, (c) patterning of the SiC/Si exposes the silicon to the atmosphere (d) high-
22 temperature annealing leads to a massive Si sublimation, resulting in the formation of an
23 anisotropic gap extending for microns.

24